ACS OMEGA

Open Access

This article is licensed under CC-BY-NC-ND 4.0

http://pubs.acs.org/journal/acsodf

Article

Biochemical Properties of CARM1: Impact on Western Blotting and Proteomic Studies

Julie Bourassa, Genevieve Paris, Laura Trinkle-Mulcahy, and Jocelyn Côté*

Cite This: *ACS Omega* 2024, 9, 40204−40213

Read Online

ACCESS | Metrics & More | Article Recommendations | Supporting Information

ABSTRACT: CARM1 is an arginine methyltransferase that has crucial roles in a number of cellular pathways and is being explored as a therapeutic target in diseases such as cancer and neurodegenerative disorders. Its deregulation at the protein level was found to have potential prognostic value, and as such, its protein levels are regularly assessed through the common practice of western blotting (WB). Our group uncovered that CARM1 has biochemical properties that complicate its analysis by standard WB sample preparation techniques. Here, we show that CARM1 has the ability to form SDS-resistant aggregates that effectively hinder gel migration in SDS-PAGE. CARM1 levels and the temperature at the denaturation step can both influence CARM1 aggregation, which prompts the use of additional measures to ensure representative detection at the protein level. We have demonstrated the formation of CARM1 aggregates in both cell and tissue extracts, making these findings an important consideration for any CARM1-related study. We also show how aggregate formation in models of CARM1 overexpression can hinder proteomic studies. Having identified factors that can induce CARM1 aggregation, we suggest alternative sample preparation techniques that allow for clear resolution of the protein in stringent denaturing conditions while avoiding aggregation.

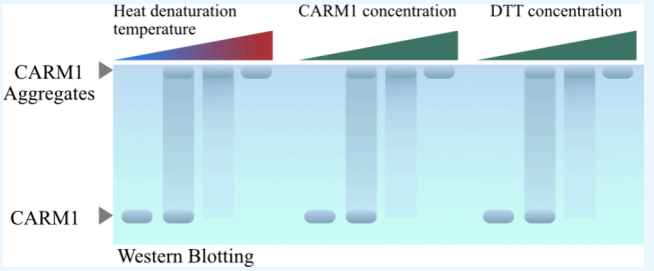

INTRODUCTION

CARM1 (Co-activator associated arginine methyltransferase) or PRMT4 is a member of the PRMT family responsible for the prevalent post-translational modification (PTM) of arginine methylation.[1,2] CARM1 is characterized as a type 1 PRMT; capable of catalyzing asymmetrical w-NG,NG dimethylation of arginine (ADMA)[1,2] through which it takes part in normal cell functions, such as epigenetics,[3,4] transcriptional regulation,[5] splicing,[5,6] cell cycle regulation,[7] and translation.[5] The methylation it imparts is broad in impact and distinctive from other PRMTs through its unique recognition motif[6,8]; its importance highlighted by the fact that the loss of CARM1 as a whole or loss of its enzymatic activity is incompatible with life.[9,10] In addition, there is abundant evidence that its deregulation is tightly associated with disease. Most notably, CARM1 has been consistently shown to be involved in cancers such as breast cancer,[11,12] ovarian cancer,[13] lung cancer,[14] and pancreatic cancer[15] among others, with interest arising from its apparent driving force toward increased disease severity as well as its potential prognostic value (Cheng et al.[12] and Qiu et al.[4]). Hence, in the recent years, an increasing amount of research effectively included CARM1 within their investigative rationale. Alike to the tendency of other proteins, CARM1 protein level is tied to protein function, and so the need to accurately assess its abundance is a necessity. For this purpose, most opt for the most prevalent proteomic and molecular biology technique of western blotting (WB).[16]

WB is most often coupled with SDS-PAGE as a universal analytical tool for protein assessment warranted by its applicability to most proteins, allowing for direct size comparison and quantification without confounding factors such as bulk or intrinsic charge. In the first step of the technique, standard practices of sample preparation call for protein denaturation by heating samples at 95 °C for 5−10 min in the presence of Laemmli buffer composed of dithiothreitol (DTT), 2-mercaptoethanol (βME), Tris−HCl, and sodium dodecyl sulfate (SDS). In this sample buffer, DTT or βME serves to break disulfide bonds, preventing the formation of covalent bonds through cysteine residues. All the while SDS, a surfactant and strong denaturant, gathers around the peptides and promotes denaturation through its hydrophobic and hydrophilic moieties.[17] During the denaturation process, SDS binds denatured proteins along their backbone and provides a uniform negative charge acting as a driving force for protein migration during SDS-PAGE. After size separation, the proteins are bound to a membrane that can

Received: July 9, 2024
Revised: September 3, 2024
Accepted: September 6, 2024
Published: September 13, 2024

© 2024 The Authors. Published by American Chemical Society

further be used for immunoblotting (IB), visualization, and quantification.

The process of sample preparation for SDS-PAGE is often inferred in the methodology of published work, leaving ambiguity in the conditions used in such a crucial step of WB. After its original definition,[18] sample preparation is understood to have variability in its practice,[19,20] as defined by user preference. As such, there is no true specification of a standard. With that being said, although there is a range of conditions belonging to the standard of procedure, these conditions have successfully been used and remain compatible with most proteins. Here, we show that these conditions do not extend to CARM1 due to their distinct biochemical properties. Standard WB conditions cause CARM1 to accumulate into SDS-resistant aggregates, which sequester and prevent CARM1 migration in SDS-PAGE. This disproportionally impacts its detection by WB, inserting error through inaccurate representation of its expression. We identify heat denaturation, CARM1 concentration, and DTT as major driving factors for aggregation formation. Further investigation into the PRMT family shows that CARM1 is not the only PRMT impacted by these biochemical properties; they also extend to PRMT1 which can aggregate albeit to a lesser extent. In both instances, increasing SDS concentrations and avoiding DTT in loading samples have mediated the interactions at the cause of aggregate formation and improved WB detection. We therefore argue that these modifications are required for sample preparations of CARM1 and PRMT1 to preserve their quantitative reliance in WB and SDS-PAGE and avoid misleading results.

METHODS

Cell Culture. Motoneuron derived cell line (MN-1) cells[21] were grown in L-glutamine free DMEM (Dulbecco's modified Eagle's medium) (09354; GIBCO) supplemented with 10% heat-inactivated FBS (fetal bovine serum) (080150; Wisent), 100 U/mL penicillin streptomycin (SV30010; Cytiva), and 2 mM of L-glutamine (25030081; GIBCO). C2C12, 293T, Hela, MCF7, and MDA-MB-231 cells were obtained from ATCC and grown in DMEM (319-015-CL; Wisent) supplemented with 10% FBS (080150; Multicell) and 100 U/mL penicillin streptomycin (SV30010; Cytiva). NIH3T3 was obtained from Dr. Livio Pellizzoni from Columbia University and cultivated as described for MN-1 cells. All cells were kept in a humidified incubator at 37 °C and 5% CO_2 and tested for mycoplasma routinely through a PCR detection kit (G238; Abm).

Mice Tissues. Animal procedures were approved by the University of Ottawa Animal Care Committee and comply with the Canadian Council on Animal care guidelines and the Animals for Research Act (protocol #: CMMb-3995).

The brains and livers of the spinal muscular atrophy SMNΔ7 mice model[22] were excised and snap frozen in liquid nitrogen before being crushed into a powder prior to sample preparation.

Plasmids and Stable Cell Lines. The human CARM1 open reading frame sequence was subcloned into the pEGFP-N1 empty vector by using the Gibson method. A site-directed mutagenesis was used to create the CARM1 E266Q catalytically inhibited mutant. The plasmids were amplified through the transformation of DH5α *E. coli* competent cells for amplification. The correct insertion, sequence, and mutation of each plasmid were validated through sequencing (Génome Québec services).

To generate stable MN-1 cells, the pEGFP-N1, pEGFP-N1 CARM1, and pEGFP-N1 CARM1 E266Q were transfected into WT MN-1 cells and selected with G418 at a concentration of 2000 μg/mL and maintained at a concentration of 200 μg/mL. The cells were sorted by flow cytometry to select for a cell population expressing GFP in comparable intensity between the three stable cell lines.

Purified Protein. Recombinant CARM1 was purchased from Active Motif (Cat# 81807).

Sample Buffers. The standard 5× sample buffer consists of 250 mM Tris−HCl pH 6.8, 10% (w/v) SDS, 0.5 M DTT, 50% (w/v) glycerol, 25% βME and 0.1% (w/v) bromophenol blue in water. The adapted 4× sample buffer consists of 200 mM Tris HCl pH 6.8, 24% (w/v) SDS, 40% (w/v) glycerol, 25% βME, and 0.1% (w/v) bromophenol blue in water.

Sample Preparation. Cells pelleted in PBS and mice tissue powder were resuspended in RIPA lysis buffer (100 mM Tris pH7.4, 100 mM NaCl, 1 mM EDTA, 1% NP-40, 0.5% (w/v) NaDOC and 0.1% (w/v) SDS in water) completed with complete protease inhibitors (04693159001, Roche) and 10 μg/mL PMSF before use. Cells were incubated on ice and vortexed intermittently for 15 min. Mice tissue powder samples were snap frozen in liquid nitrogen and vortexed, repetitively, for 1 h. Samples were centrifuged for 15 min at 4 °C at 13,000 rpm, and the supernatant was collected. The protein concentration was determined through a Bradford Assay (DC protein assay, Biorad). These concentrations were considered for the preparation of samples, mixing with the specified samples buffer, and heat denatured at 95 °C for 8 min unless otherwise specified.

SDS-PAGE. The samples were resolved by SDS-PAGE with gels made of a 4% acrylamide stacking gel layer followed by a 10% acrylamide resolving gel and transferred to a nitrocellulose membrane, making sure to preserve the stacking gel. The membranes were blotted in 5% nonfat milk in PBS-T (with 0.05% Tween-20) prior to IB.

Antibodies and IB. For WB, the antibodies used were; CARM1 from Cell Signaling Technologies (3379S) 1:1000, GFP from ChromoTek (3H9-100) 1:1000, PRMT2 from Proteintech (66885-1-Ig) 1:1000, PRMT6 from Bethyl (A300-929A) 1:3000, PRMT7 form Cell Signaling Technologies (14762s) 1:1000, GAPDH from BioLegend (MMS-580S) 1:3000 and α-Tubulin from Millipore Sigma (T6199) 1:10,000. The PRMT5 and PRMT1 antibodies were made in house. The antibodies were diluted in a gelatin blocking buffer for IB. Li-Cor IRDye 680LT Goat anti-Mouse IgG (926-68020) and IRDye 800CW Donkey anti-Rabbit IgG Secondary Antibody (926-32213) fluorescent secondary antibodies or horseradish peroxidase (HRP) conjugate secondary antibodies and HRP substrate (Millipore) were used to visualize IB.

Statistical Analysis. All statistical analysis and graphs were done with GraphPad Prism software (Version 10.2.2 (397)).

RESULTS

Under standard SDS-PAGE and WB conditions, we found that the CARM1 immunoblot (IB) signal has the potential to mislead interpretation of band intensity. In MN-1 cells stably expressing GFP tagged CARM1 or CARM1 E266Q (catalytically inactive mutant[6]) fusion proteins, we report that running increasing amounts of protein lysate per well correlated with an increasing loss of endogenous and exogenous CARM1 signal at their predicted molecular weight (63 and 90 kDa, respectively) (Figure 1A, top panels). The loss of the anticipated band

https://doi.org/10.1021/acsomega.4c06360
ACS Omega 2024, 9, 40204−40213

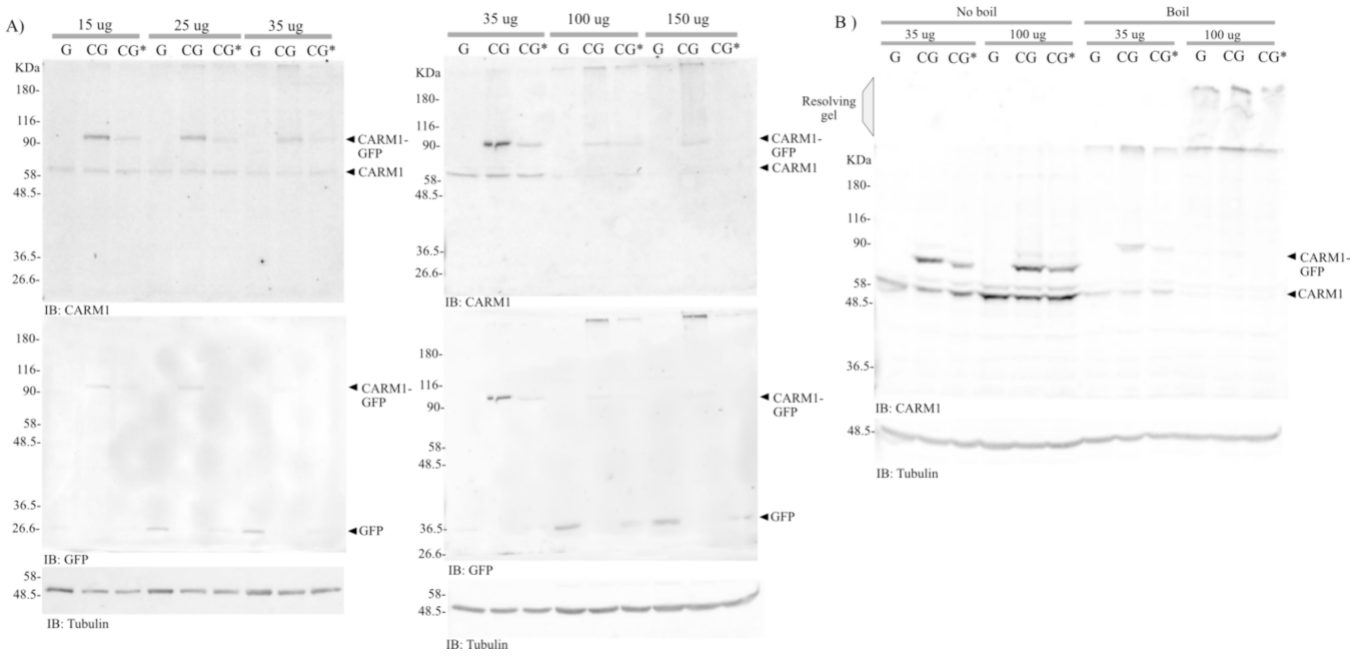

Figure 1. CARM1 aggregation is dependent on the amount of protein sampled. Aggregation of CARM1 with loading samples of increasing protein amount (A,B), with or without heat denaturation (B). Protein lysates were prepared from MN-1 cells stably expressing EGFP (G), CARM1-EGFP (CG) and CARM1/E266Q-EGFP (CG*), mixed with standard sample buffer, and either heated for 8 min at 95 °C (boil) or incubated at room temperature (no boil) before resolving by SDS-PAGE and immunoblotted. IB; immunoblot.

correlated with the increased signal of a band at a larger size (>180 kDa), or at the junction between the resolving and running gel. The same pattern in signal was observed with using GFP IB as a secondary validation (Figure 1A, bottom panels). This concurrent shift suggests that CARM1 can assemble into large protein aggregates surpassing the maximum threshold for gel migration. Given that this trend is observed for both endogenous and exogenous CARM1, it is unlikely that the aggregates are an artifact of the constructs and additionally argues against the requirement of CARM1 catalytic activity for aggregation. We therefore concluded that the size shift of the protein signal consists of CARM1 aggregation which prevents its migration through the gel. Given this property, only considering the predicted signal would erroneously imply an inverse correlation between detectable CARM1 protein levels and total protein amount for the same sample. Therefore, under these standard conditions CARM1 protein signal should not be interpreted at face value.

To resolve the events leading to CARM1 aggregation, the effect of the temperature was investigated. Standard procedure of sample preparation (as shown in Figure 1A) relies on the heating of samples at 95 °C for 5−10 min in the presence of sample buffer for protein denaturation.[19,20] Heat is a known factor in protein aggregation.[23] To test if high denaturing temperatures are a driving factor for CARM1 aggregation, the samples were exposed to lower temperatures for increased amounts of time with the aim of achieving protein denaturation while avoiding aggregation (Supplementary Figure 1A). The resulting blots reveal that CARM1's signal remained visible at its expected molecular weight but streaked from the top of the gel, acting as an intermediate between proper migration and complete aggregation. This was confirmed with GFP IB which matched CARM1's streaked signal pattern. In addition, the proportion of CARM1 migrating at its expected size was inversely proportional to amount of total protein loaded (as shown in Figure 1A) and temperature, indicating a dependence on both temperature and protein concentration for aggregation.

With evidence that heat denaturation contributed to CARM1 aggregation, CARM1's ability to migrate through the gel without heat denaturation was tested. Here (Figure 1B), the samples are incubated at room temperature in standard sample buffer before running on a gel. CARM1 was able to migrate properly into the gel without detectable aggregations. As expected, CARM1 runs lower than its expected size due to its partially denatured state, most likely adopting a more compact conformation. The doublet is indicative that a subset of the CARM1 protein was able to fully denature without the need for heat denaturation. Interestingly, CARM1 aggregates are so large that they can barely migrate into the stacking buffer (4% acrylamide), reflecting widespread interlinking of the CARM1 proteins. Hence, to avoid CARM1 aggregation and allow complete protein migration, heat denaturation must be avoided.

To test if CARM1 aggregation is dependent on the protein concentration rather than the total protein amount loaded in a single well, samples containing equal amounts of protein in different final volumes were prepared (Figure 2A). Decreasing total protein concentration led to a decrease in aggregation.

To test the requirements needed for CARM1 aggregation, purified recombinant CARM1 was used in WB analysis with both heat-denaturing and nonheat-denaturing methods of sample preparation (Figure 2B). The ability of the purified recombinant CARM1 protein to form aggregates shows that the presence of other proteins is not required for CARM1 aggregation. This points toward an intrinsic ability to form aggregates.

Noticeably, aggregates also formed in the nonheat denatured sample, which differs from what was seen in cell culture and mice tissues. These results imply a critical concentration

https://doi.org/10.1021/acsomega.4c06360
ACS Omega 2024, 9, 40204−40213

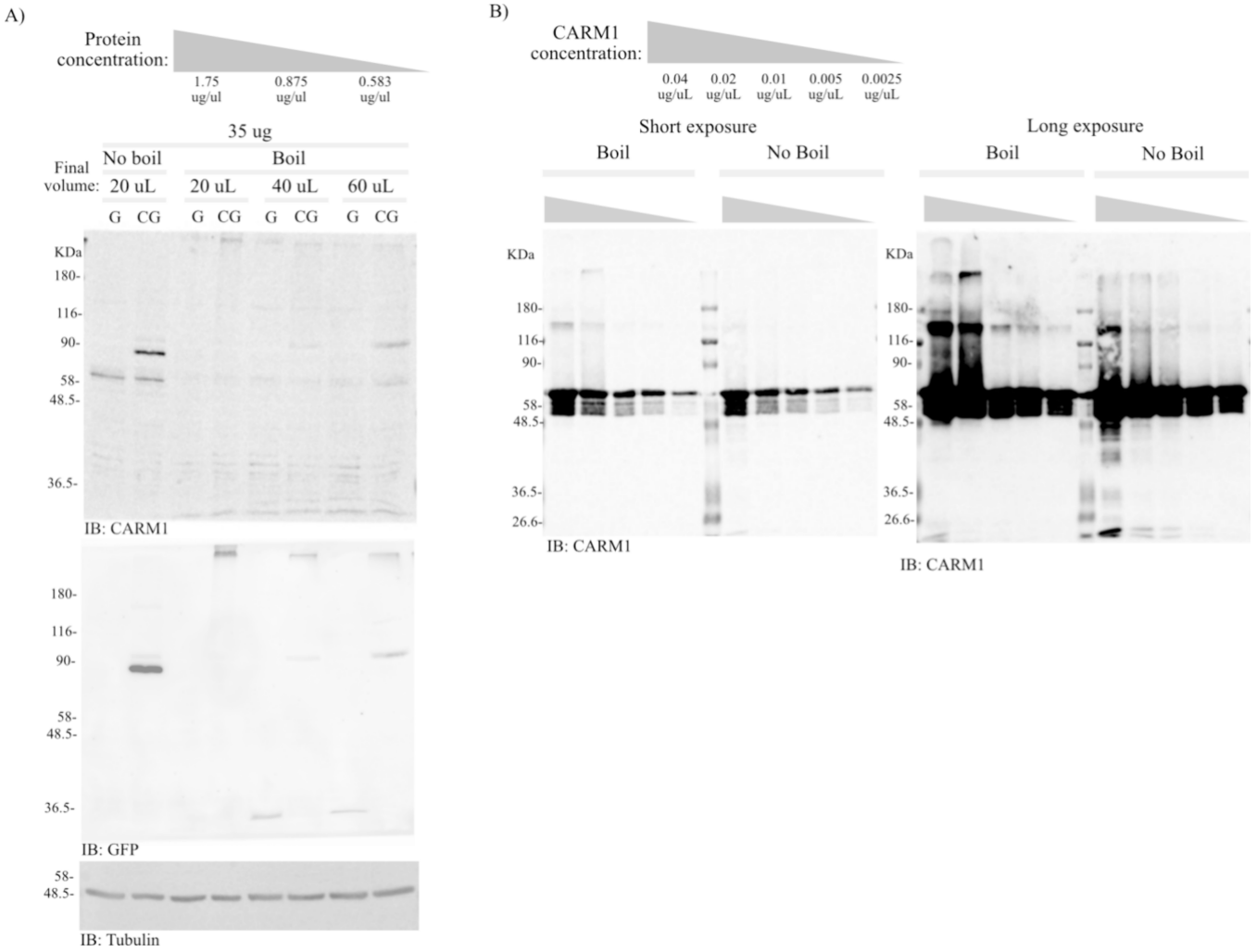

Figure 2. CARM1 aggregation is dependent on its concentration. Protein lysates of MN-1 cells stably expressing EGFP (G) and CARM1-EGFP (CG) prepared in samples of equal protein amounts in differing volumes (A). CARM1 full-length recombinant purified protein was prepared in samples of equal volume (B). The samples were mixed with standard sample buffer and heated for 8 min at 95 °C (boil) or incubated at room temperature (no boil) before running by SDS-PAGE and immunoblotted. IB; immunoblot.

threshold beyond which CARM1 will aggregate regardless of temperature and suggest that CARM1's own concentration within the sample, rather than total protein concentration, is a predominant factor contributing to aggregation. This is put in evidence in Figure 2B where CARM1 recombinant protein was able to form aggregates at much lower total protein concentrations than shown in total cell lysate (Figure 2A).

To test if heat-dependent CARM1 aggregation is relevant in other models, the ability of CARM1 to form aggregation was evaluated in various cell lines and mice tissues. In all cell lines and tissue types tested so far, which include NIH3T3, NSC34, C2C12, HEK293T, HeLa, MCF7, MDA-MB-231 (Figure 3A), and MN-1 cell lines (Figure 1) as well as mouse brain and liver tissues (Figure 3B and Supplementary Figure 1B), CARM1 aggregates were detected. In addition, consistent with what was shown previously, CARM1 aggregation in mice brain and liver tissues (Figure 3B) formed aggregation in a protein concentration- and temperature-dependent fashion. This supports the idea that CARM1 aggregation is not limited to a specific cell type and suggests a widespread occurrence through a conserved mechanism.

The data shown so far suggest that CARM1 aggregation is an artifact of sample preparation that has the potential to alter the biological interpretation of results and invalidate their reliability for protein quantification. As shown, avoiding heat denaturation in cell lines or mice tissues allowed proper migration of CARM1 by SDS-PAGE. We therefore aimed to compare the intensity of the CARM1 signal between the two methods of sample preparation in a range of protein concentrations.

In both mice brain and liver tissues and across all protein concentrations, the normalized nonheat denatured samples had a significantly stronger CARM1 signal when compared to their heat denatured equivalent (Figure 3B and Supplementary Figure 1B). As reflected in Figure 1A, the difference in signal was further exorbitated with increasing protein concentration. This is consistent with our proposed model where aggregation sequesters CARM1 and prevents its migration in a protein concentration-dependent manner. That being said, even the CARM1 signal in the least concentrated samples (15 mg, or 0.43 $\mu g/\mu L$) was statistically different compared to their nonheat denatured equivalent, indicating that limiting protein concentration in samples is not enough to completely prevent a shift in quantification.

Contrastingly, GAPDH and PRMT7 quantifications remained proportional in either method of sample preparation,

https://doi.org/10.1021/acsomega.4c06360
ACS Omega 2024, 9, 40204−40213

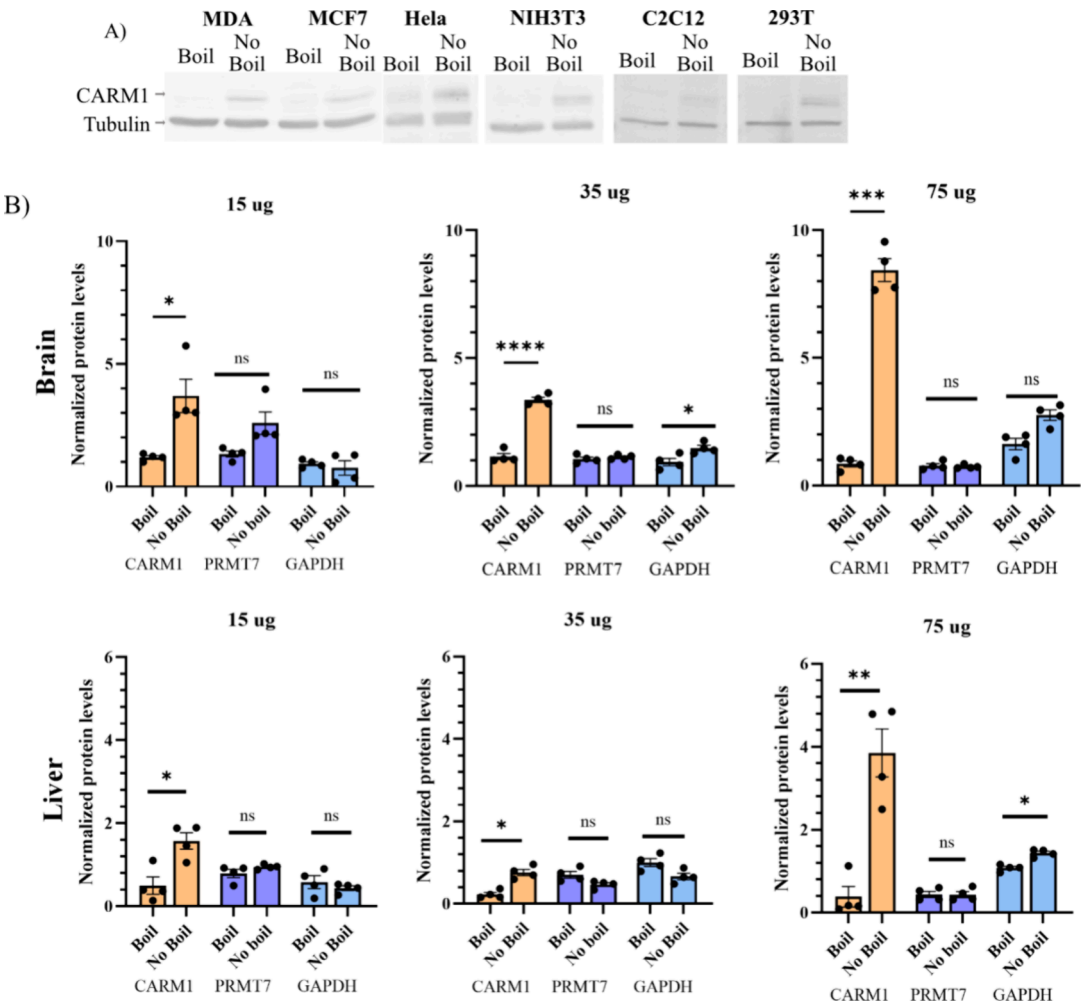

Figure 3. CARM1 aggregation occurs in multiple models. (A) Protein lysate of MDA-MB-231 (MDA), MCF7, Hela, NIH3T3, C2C12, and 293T cell lines prepared in samples containing 35 μg in a final volume of 30 μL. (B) Protein lysate of mice brain and liver tissue prepared in samples containing the indicated protein amount in a final volume of 40 μL. Values were normalized to total protein (Ponceau staining). The samples were heat denatured at 95 °C for 8 min (boil) or incubated at room temperature (no boil) prior to SDS-PAGE. Statistics; paired t test, $P < 0.05$, error bars show SEM, $N = 4$.

tissue type, and protein range (Figure 3B). Here, GAPDH is used because of its extensive use as a loading control in WB without reports of aggregations impeding its migration. PRMT7, a protein in the same family as CARM1 with no detectable aggregation (Figure 4F), is used to contrast CARM1's own ability to do so. Overall, the data suggest that CARM1 is disproportionately impacted by sample preparation and demonstrate that the standard procedure of sample preparation in WB techniques inserts error in CARM1 protein quantifications, therefore making standard sample preparation unsuited for its study.

The data shown so far suggest that CARM1's ability to form aggregates is a consequence of its own structural features. That being said, all members of the PRMT family are known to have a largely conserved catalytic core. We set out to determine if heat denaturation-dependent aggregation also prevented gel migration of other canonical PRMTs. PRMT8 was excluded from this study because of its transmembrane nature, which differentiates it from the other cytosolic or nuclear PRMTs. PRMT3 was also excluded due to its low expression in the same cell model. GAPDH was used to normalize PRMT2 instead of α-Tubulin because they are of equal size and have overlapping signals. Interestingly, the impact of heat denaturation did not significantly impact PRMTs (Figure 4), for the exception of PRMT1, PRMT5, and of course CARM1 (Figure 4A,C,D). While statistically significant, the protein signal of PRMT5 remains comparable in its quantification, while PRMT1's doubles when avoiding heat denaturation. PRMT1 aggregates at high molecular weights were also observed after heat denaturation of samples in a manner resembling that seen with CARM1. It is worth noting that no aggregates were detected for the other PRMTs (Figure 4B,D–F). The fact that other PRMTs remain largely unaffected by the method of sample preparation attests to the uniqueness of CARM1 and PRMT1 even among their paralogous and structurally conserved counterparts.

The data indicate that the minimum stringency required to prevent CARM1 aggregation is above what is provided by standard loading buffers. SDS is universally used in loading buffers for its ability to drive forward protein unfolding and to mediate hydrophobic interactions. To this effect, the standard SDS concentration in Laemmli buffer is typically kept at 2%. Since these conditions do not extend to CARM1, we reasoned that increasing SDS availability might offer the stringency required to mediate the interactions at their cause. As described previously, the expression of GFP tagged CARM1

https://doi.org/10.1021/acsomega.4c06360
ACS Omega 2024, 9, 40204−40213

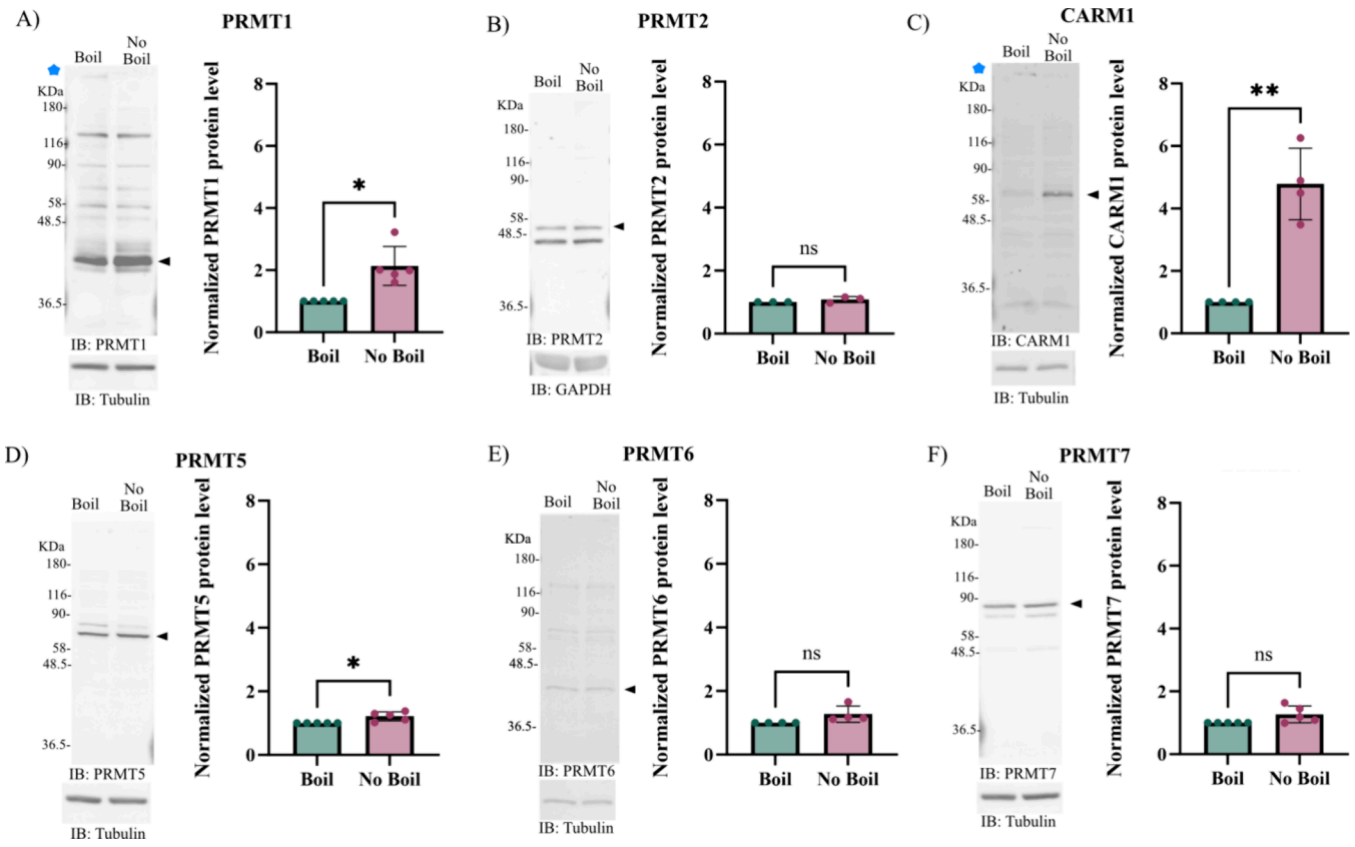

Figure 4. Aggregation of canonical PRMT proteins. (A–F) Immunoblots of canonical PRMTs in protein lysate of MN-1 cells prepared in samples of 35 μg in 30 μL in heat-denaturing conditions (8 min at 95 °C, termed boil) or incubated at room temperature (termed no boil) followed by SDS-PAGE and western blotting. Arrowhead indicates the predicted band of each PRMT. Blue start indicates detectable aggregates. Statistics; paired *t* test, $P < 0.05$, error bars show SD, $N = 3–5$.

is used as a secondary mean of IB validation. It is worth noting that different migration heights of CARM1-GFP suggest incomplete or partial denaturation dependent on the sample preparation method. Interestingly, the SDS concentration had to be tripled before CARM1 aggregation was noticeably reduced. Even so, at a final concentration of 6% SDS, CARM1 aggregates were still present, albeit to a much lesser extent (Figure 5A). Further increasing SDS concentrations to 10% provided no extra benefit compared to the 6% SDS (Figure 5A). These results suggest that aggregations are driven by hydrophobic interactions.

To test the stability of CARM1 aggregates, samples were heat denatured in 2% SDS to promote the formation of aggregates, after which the SDS concentration was adjusted to a final concentration of 6% and either incubated at room temperature or heat denatured once more (Figure 5A). In both cases, increasing SDS concentration to 6% after aggregate formation was not able to resolve aggregation, displaying their strong resistance to SDS, and pointing toward a different mechanism also contributing to CARM1 aggregation.

While the driving force of aggregates seems to be of hydrophobic nature, their surprising stability to high SDS concentrations once formed suggests a potential covalent interaction between CARM1 proteins. To test if disulfide bonds are involved in the aggregations, samples were treated in a range of DTT concentrations prior to SDS-PAGE. We reasoned that increasing DTT concentrations would resolve the aggregations should they be disulfide bond dependent. Surprisingly, the increase of DTT concentration further prevented normal migration of CARM1 when heat denatured (Figure 5B). While suggesting that disulfide bonds are involved in aggregation, it also concludes that this is not done in a contributive manner. Since higher SDS concentrations are better at mediating aggregations, its ability to rescue aggregation in a high DTT concentration context was tested (Figure 5C). A concentration of 6% SDS was able to resolve the aggregations, meaning that the root cause leading to aggregation following DTT treatment in heat-denaturing conditions was mediated by SDS, and therefore of a noncovalent nature.

The data shown so far point toward the use of higher concentrations of SDS in the absence of DTT for a more accurate representation of the CARM1 protein level. A sample buffer suited to CARM1's properties was therefore prepared and compared to standard sample buffer (Figure 5D). The use of the adapted buffer (6% SDS, no DTT) significantly increased the proportion of CARM1 properly migrating to the gel in heat-denaturing conditions, leading to a complete recovery of CARM1 protein levels as compared to its nonheat denatured condition. This makes the use of an adapted sample buffer required for the accurate assessment of CARM1 protein levels.

Importantly, the impact of DTT and high SDS concentrations observed for CARM1 extended to PRMT1 (Figure 5B,C), further pointing toward a common mechanism of aggregation. The use of an adapted sample buffer (Figure 5D) was beneficial for PRMT1 detection, albeit to a lesser significance due to a lower prevalence of aggregates. The use

https://doi.org/10.1021/acsomega.4c06360
ACS Omega 2024, 9, 40204–40213

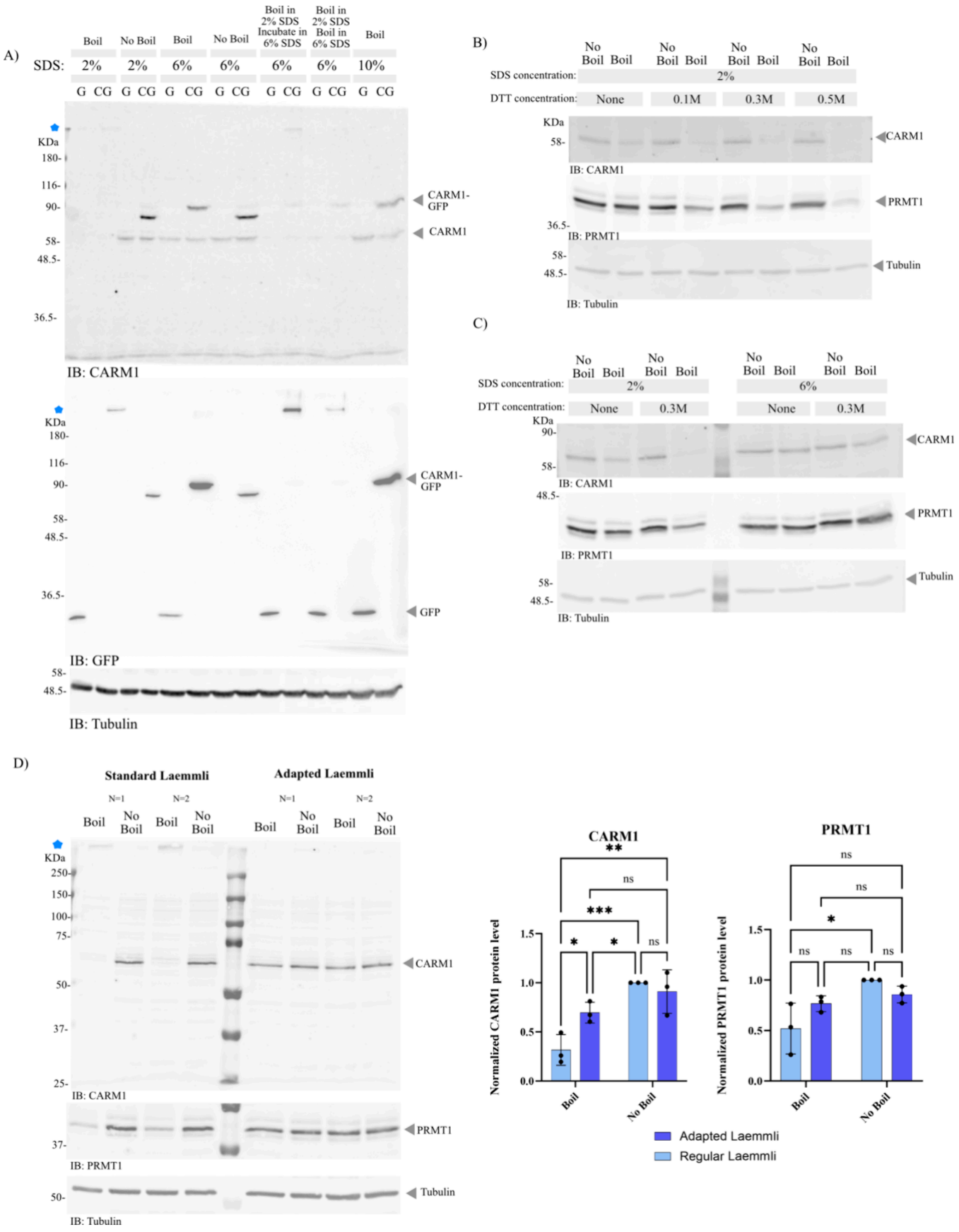

Figure 5. PRMT1 and CARM1 aggregates are inhibited by SDS at formation and promoted by DTT. (A) Protein lysate samples of stable MN-1 cells expressing GFP (G) or CARM1-GFP (CG) containing 35 μg in 30 μL prepared and either heat denatured or incubated at room temperature with an increasing range of SDS. For samples with two SDS treatments, the concentration of SDS was increased from an initial 2−6% after the first

https://doi.org/10.1021/acsomega.4c06360
ACS Omega 2024, 9, 40204−40213

Figure 5. continued

heat denaturation step, prior to another heat denaturation or incubation at room temperature step. Samples of MN-1 WT protein lysate containing 35 μg of 30 μL prepared and either heat denatured or incubated at room temperature with increasing range of DTT (B) or DTT and SDS (C). (D) Using an adapted sample buffer (purple) with 6% SDS and no DTT, samples were prepared and heat denatured or incubated at room temperature prior to SDS-PAGE, WB and quantification. $N = 4$. Statistics; two-way ANOVA, error bars show SD. All heat denaturation steps were done for 8 min at 95 °C. IB; immunoblot. Blue start indicates detectable aggregates.

of an adapted sample buffer is therefore recommended for PRMT1 to ensure more accurate results.

DISCUSSION

WB is a standard procedure and indisputably a necessary tool in proteomics and molecular biology, with the advantage of applicability to most proteins. Here, we show that CARM1 does not fall within this category, with prominent aggregation preventing its detection by conventional methods. We have shown the aggregates to be dependent on temperature at the protein denaturation step as well as CARM1's own protein concentration. Aggregates are also widespread to a range of models, suggesting their ubiquitous occurrence. As such, it is likely that these factors are unknowingly introducing inaccuracies in CARM1's study.

There is a lot of interest in the evaluation of CARM1 protein levels in cancer as its overexpression was found in many tumors when compared to healthy tissue, suggesting a role in cancer pathogenesis.[4] As such, modulating CARM1 expression as models of overexpression or knockdown in either a cell or mice model is a strategy often used in investigative research. It is therefore a requirement that it be assessed accurately without confounding factors.

Considering this, we set out to investigate the cause of the aggregates, as well as defining conditions that allow accurate CARM1 quantification in SDS-PAGE with heat denaturation. Increasing SDS concentrations to 6%; or three times the conventional availability of SDS, was successful preventing most of the aggregations. The successful use of SDS points toward hydrophobic interactions as being the primary driving force to aggregate formation. Surprisingly, DTT treatment led to stronger aggregation, demonstrating that disulfide bonds present in the protein are protective against aggregation and beneficial for CARM1 gel migration. Combining both findings by increasing SDS and removing DTT from standard loading buffer provides a complete rescue of CARM1 protein migration and an alternative preparation method suited for CARM1's study.

These findings are consistent with a model in which a hidden hydrophobic core of CARM1 is at the cause of the aggregates but is shielded in the presence of disulfide bonds in its native state. When broken, the hydrophobic core is revealed and acts as a nucleation site to irreversibly sequester the CARM1 protein into aggregates. When left intact, the bonds shield the hydrophobic core and allow for denaturation and CARM1 migration without exposure to the nucleation site. In either scenario, high SDS availability seems to have the ability to mediate hydrophobic moieties other than those shielded by disulfide bonds.

Even if the capabilities of SDS to denature proteins are well recorded, the kinetics outlining its mechanism remain unelucidated.[24] Transmembrane proteins are well established as having the ability to form aggregates through their hydrophobic core that can unfold and initiate misfolding.[25] They also encompass most reports for aggregation, implying that only the transmembrane protein has this ability. This study argues against this general standpoint and expands this premise to unidentified proteins in the process of sample preparation. This highlights the need for more biochemical studies focusing on the structural basis that leads to proteins to be excluded from the traditional method of sample preparation for SDS-PAGE and WB analysis.

CARM1 is not unique in its ability to form aggregates, as demonstrated with PRMT1, but it stands out in terms of the degree of bias aggregates introduce. Given that PRMTs share a conserved catalytic core, this argues that the property of aggregation should be allotted to CARM1 through its unique structural components. In the same line of thought, the C-terminal domain of CARM1 is unique among PRMTs, and well-known for its unstructured conformation and potential hindrance in CARM1 proteomic studies. The particularity of the domain has been suggested to be causing difficulties with X-ray crystallography methods.[26] Most successful X-ray crystallography structures reported so far have either found the C-terminal domain to have low electron density suggesting a disordered state or excluded it due to difficulties at its resolution.[26] Additionally, full-length recombinant CARM1 purification is reportedly difficult due to its propensity to accumulate into inclusion bodies as insoluble aggregates.[27] It is plausible that the unstructured C-terminal domain of the protein is at cause for all these challenges; however, more needs to be done before reaching this conclusion.

There are no reports of physiological relevance for CARM1 aggregates. Nevertheless, it cannot be ruled out that CARM1's ability to drastically alter its hydrophobicity might be relevant to protein function given its susceptibility to aggregate. Hydrophobicity and electrostatic interactions are key elements for the liquid−liquid phase separation of membraneless organelles. These include paraspeckles, to which a pool of CARM1 has been shown to localize.[28,29] It is possible that CARM1's structure is modified to control its subcellular localization to such organelles.

In any case, bypassing the effects of aggregation is in the best interest of proteomic studies used for CARM1's understanding. As mentioned, aggregations are dependent on CARM1's own concentration. This is of relevance when working with a model of CARM1 overexpression, as is often the case in exploratory research. It is also unknown if all isoforms of CARM1 are affected equally, which may introduce another layer of variability when not considered.

The use and effect of other reducing agents such as βME have yet to be evaluated, but they may provide additional options for the prevention of CARM1 aggregate formation. While our adapted sample buffer does contain a reducing agent, it should also be noted that the complete absence of reducing agents could lead to the formation of non-CARM1 aggregates.

As demonstrated, CARM1 aggregation is dependent on a variety of factors which may vary with an experiment's specific conditions. Therefore, the presence of aggregates should be

https://doi.org/10.1021/acsomega.4c06360
ACS Omega 2024, 9, 40204−40213

empirically evaluated, with a comparison of heat denatured and nonheat denatured CARM1 signals as an additional control. It should be understood that proteolytic activity, normally negated during heat denaturation,[30] is not addressed without heat denaturation, so we advise the use of parallel protease inhibition as an additional measure.

The use of the adapted sample described here is strongly recommended for CARM1 SDS-PAGE under heat-denaturing conditions without which the introduction of aggregates is bound to mislead result interpretation. As a whole, these findings should be considered in any study involving CARM1 and kept in mind in the interpretation of the results published so far.

Protein Accession IDs. CARM1: Q86X55 (human), CARM1: Q9WVG6 (mouse); PRMT1: Q9JIF0; PRMT2: Q9R144; PRMT3: Q922H1; PRMT5: Q8CIG8; PRMT6: Q6NZB1; PRMT7: Q922X9; PRMT8: Q6PAK3; GAPDH: P16858; Tubulin: P68368.

■ ASSOCIATED CONTENT

Supporting Information

The Supporting Information is available free of charge at https://pubs.acs.org/doi/10.1021/acsomega.4c06360.

Brain and liver tissues full immunoblots (PDF)

■ AUTHOR INFORMATION

Corresponding Author

Jocelyn Côté − *Department of Cellular and Molecular Medicine, Faculty of Medicine and Center for Neuromuscular Disease, Faculty of Medicine, University of Ottawa, Ottawa, Ontario K1H 8M5, Canada*; Email: jcote@uottawa.ca

Authors

Julie Bourassa − *Department of Cellular and Molecular Medicine, Faculty of Medicine, University of Ottawa, Ottawa, Ontario K1H 8M5, Canada*; orcid.org/0000-0002-3053-1203

Genevieve Paris − *Department of Cellular and Molecular Medicine, Faculty of Medicine, University of Ottawa, Ottawa, Ontario K1H 8M5, Canada*

Laura Trinkle-Mulcahy − *Department of Cellular and Molecular Medicine, Faculty of Medicine, University of Ottawa, Ottawa, Ontario K1H 8M5, Canada; Ottawa Institute of Systems Biology, University of Ottawa, Ottawa, Ontario K1N 6N5, Canada*

Complete contact information is available at: https://pubs.acs.org/10.1021/acsomega.4c06360

Author Contributions

J.B. performed the experiments. All authors analyzed and interpreted the data. J.B. wrote the first draft, which was reviewed by all authors for feedback. All authors read and approved the final manuscript.

Funding

We thank CIHR (GR000687) and CureSMA (GR006339) for their support.

Notes

The authors declare no competing financial interest.

■ ACKNOWLEDGMENTS

We thank Dr. M. T. Bedford for his gift of a CARM1 plasmid that was used to generate the plasmids used in this study. We thank Andréanne Didillon for helpful conversation throughout this project. The University acknowledges and respects that it stands on unceded Algonquin territory.

■ REFERENCES

(1) Bedford, M. T.; Clarke, S. G. Protein arginine methylation in mammals: who, what, and why. *Mol. Cell* **2009**, *33*, 1−13.

(2) Herrmann, F.; Pably, P.; Eckerich, C.; Bedford, M. T.; Fackelmayer, F. O. Human protein arginine methyltransferases in vivo−distinct properties of eight canonical members of the PRMT family. *J. Cell Sci.* **2009**, *122*, 667−677.

(3) Van Haren, M. J.; et al. Transition state mimics are valuable mechanistic probes for structural studies with the arginine methyltransferase CARM1. *Proc. Natl. Acad. Sci. U. S. A.* **2017**, *114*, 3625−3630.

(4) Qiu, Y.; et al. Systematic pan-cancer landscape identifies CARM1 as a potential prognostic and immunological biomarker. *BMC Genom. Data* **2022**, *23*, 7.

(5) Wei, H. H.; et al. A systematic survey of PRMT interactomes reveals the key roles of arginine methylation in the global control of RNA splicing and translation. *Sci. Bull. (Beijing)* **2021**, *66*, 1342−1357.

(6) Cheng, D.; Côté, J.; Shaaban, S.; Bedford, M. T. The Arginine Methyltransferase CARM1 Regulates the Coupling of Transcription and mRNA Processing. *Mol. Cell* **2007**, *25*, 71−83.

(7) Fujiwara, T.; et al. CARM1 Regulates Proliferation of PC12 Cells by Methylating HuD. *Mol. Cell. Biol.* **2006**, *26*, 2273−2285.

(8) Shishkova, E.; et al. Global mapping of CARM1 substrates defines enzyme specificity and substrate recognition. *Nat. Commun.* **2017**, *8*, 15571.

(9) Kim, D.; et al. Enzymatic activity is required for the in Vivo functions of CARM1. *J. Biol. Chem.* **2010**, *285*, 1147−1152.

(10) Yadav, N.; et al. Specific Protein Methylation Defects and Gene Expression Perturbations in Coactivator-Associated Arginine Methyltransferase 1-Deficient Mice. *Proc. Natl. Acad. Sci. U. S. A.* **2003**, *100*, 6464−6468.

(11) Frietze, S.; Lupien, M.; Silver, P. A.; Brown, M. CARM1 regulates estrogen-stimulated breast cancer growth through up-regulation of E2F1. *Cancer Res.* **2008**, *68*, 301−306.

(12) Cheng, H.; et al. Overexpression of CARM1 in breast cancer is correlated with poorly characterized clinicopathologic parameters and molecular subtypes. *Diagn. Pathol.* **2013**, *8*, 129.

(13) Karakashev, S.; et al. CARM1-expressing ovarian cancer depends on the histone methyltransferase EZH2 activity. *Nat. Commun.* **2018**, *9*, 631.

(14) O'Brien, K. B.; et al. CARM1 is required for proper control of proliferation and differentiation of pulmonary epithelial cells. *Development* **2010**, *137*, 2147−2156.

(15) Wang, Y. P.; et al. Arginine Methylation of MDH1 by CARM1 Inhibits Glutamine Metabolism and Suppresses Pancreatic Cancer. *Mol. Cell* **2016**, *64*, 673−687.

(16) Mishra, M.; Tiwari, S.; Gomes, A. V. Protein purification and analysis: Next generation western blotting techniques. *Expert Review of Proteomics* vol. *14* 1037−1053 Preprint at (**2017**).

(17) Krainer, G.; et al. SDS-induced multi-stage unfolding of a small globular protein through different denatured states revealed by single-molecule fluorescence. *Chem. Sci.* **2020**, *11*, 9141−9153.

(18) Laemmli, U. K. Cleavage of Structural Proteins during the Assembly of the Head of Bacteriophage T4. *Nature 1970 227:5259* **1970**, *227*, 680−685.

(19) Kurien, B. T.; Scofield, R. H. Common artifacts and mistakes made in electrophoresis. *Methods Mol. Biol.* **2012**, *869*, 633.

(20) Litovchick, L. Preparing Whole-Cell Lysates for Immunoblotting. *Cold Spring Harb. Protoc.* **2018**, *2018*, No. 098400.

(21) Salazar-Grueso, E. F.; Kim, S.; Kim, H. Embryonic mouse spinal cord motor neuron hybrid cells. *NeuroReport* vol. *2* 505−508 Preprint at (**1991**).

(22) Le, T. T.; et al. SMNΔ7, the major product of the centromeric survival motor neuron (SMN2) gene, extends survival in mice with spinal muscular atrophy and associates with full-length SMN. *Hum. Mol. Genet.* **2005**, *14*, 845−857.
(23) Ng, Y. K.; Tajoddin, N. N.; Scrosati, P. M.; Konermann, L. Mechanism of Thermal Protein Aggregation: Experiments and Molecular Dynamics Simulations on the High-Temperature Behavior of Myoglobin. *J. Phys. Chem. B* **2021**, *125*, 13099−13110.
(24) Bhuyan, A. K. On the mechanism of SDS-induced protein denaturation. *Biopolymers* **2010**, *93*, 186−199.
(25) Sagné, C.; Isambert, M.-F.; Henry, J.-P.; Gasnier, B. SDS-Resistant Aggregation of Membrane Proteins: Application to the Purification of the Vesicular Monoamine Transporter. *Biochem. J.* **1996**, *316*, 825−831.
(26) Troffer-Charlier, N.; Cura, V.; Hassenboehler, P.; Moras, D.; Cavarelli, J. Functional insights from structures of coactivator-associated arginine methyltransferase 1 domains. *EMBO J.* **2007**, *26*, 4391−4401.
(27) Chumanov, R. S.; Kuhn, P. A.; Xu, W.; Burgess, R. R. Expression and purification of full-length mouse CARM1 from transiently transfected HEK293T cells using HaloTag technology. *Protein Expr Purif* **2011**, *76*, 145−153.
(28) Hupalowska, A.; et al. CARM1 and Paraspeckles Regulate Pre-implantation Mouse Embryo Development. *Cell* **2018**, *175*, 1902−1916.
(29) Hu, S.-B.; et al. Protein arginine methyltransferase CARM1 attenuates the paraspeckle-mediated nuclear retention of mRNAs containing IRAlus. *Genes Dev.* **2015**, 630−645.
(30) Pringle, J. R. Methods for avoiding proteolytic artefacts in studies of enzymes and other proteins from yeasts. *Methods Cell Biol.* **1975**, *12*, 149−184.

https://doi.org/10.1021/acsomega.4c06360
ACS Omega 2024, 9, 40204−40213